Syndecan-1 Stimulates Adult Neurogenesis in the Mouse Ventricular-Subventricular Zone after Injury

Marc-André Mouthon, Lise Morizur, Léa Dutour, Donovan Pineau, Thierry Kortulewski, François D. Boussin

Syndecan-1 stimulates adult neurogenesis in the mouse ventricular-subventricular zone after injury

Marc-André MOUTHON*[1], Lise MORIZUR, Léa DUTOUR, Donovan PINEAU, Thierry KORTULEWSKI, François D. BOUSSIN*

Université de Paris and Université Paris-Saclay, Inserm, LRP/iRCM/IBFJ CEA, UMR Stabilité Génétique Cellules Souches et Radiations, F-92265, Fontenay-aux-Roses, France.

*Correspondence to:

Dr. Marc-André MOUTHON

marc-andre.mouthon@cea.fr

Dr François BOUSSIN

francois.boussin@cea.fr

Keywords:

Neurogenesis, neural stem cells, quiescence, cell cycle, aging, syndecan-1.

[1] Lead Contact

Summary

The production of neurons from neural stem cells (NSCs) persists throughout life in the mouse ventricular-subventricular zone (V-SVZ). We have previously reported that NSCs from adult V-SVZ are contained in cell populations expressing the carbohydrate SSEA-1/LeX, which exhibit either characteristics of quiescent NSCs (qNSCs) or of actively dividing NSCs (aNSCs) based on the absence or the presence of EGF-receptor, respectively. Using the FUCCI-Cdt1 transgenic mice to mark cells in G_0/G_1phase of the cell cycle, we uncovered a subpopulation of qNSCs which were primed to enter the cell cycle *in vitro*. Besides, we found that treatment with Syndecan-1, a Heparan Sulfate Proteoglycan involved in NSC proliferation, hastened the division of qNSCs and increased proliferation of aNSCs shorthening their G_1 phase *in vitro*. Furthermore, administration of Syndecan-1 ameliorated the recovery of neurogenic populations in the V-SVZ after radiation-induced injury providing potential cure for neurogenesis decline during brain aging or after injury.

Introduction

The generation of neurons, astrocytes and oligodendrocytes persists throughout life in specific regions of the mammalian brain and contributes to neural plasticity through rewiring, refreshing of established networks and maintenance of cognition (Kempermann et al., 2018). Remarkably, two main regions of the forebrain exhibit germinative potentials, namely the subgranular zone of the dentate gyrus in the hippocampus and the ventricular-subventricular zone (V-SVZ) (Obernier and Alvarez-Buylla, 2019). Adult neurogenesis within the V-SVZ is insured by neural stem cells (NSCs), or type B cells, that enter the cell cycle then successively give rise to transit amplifying cells (type C) and neuroblasts (type A) which differentiate into neurons once they have reached the olfactory bulbs (Obernier and Alvarez-Buylla, 2019).

In the adult brain, NSCs are contained in two populations of quiescent (qNSCs) and active NSCs (aNSCs) with different cell cycle features (Codega et al., 2014; Daynac et al., 2013). Particularly, owing their high proliferative capacity, proliferating aNSCs are rapidly eliminated in the V-SVZ after anti-mitotic treatment whereas qNSCs resist then re-entering the cell cycle to insure progressive recovery of neurogenesis (Codega et al., 2014; Daynac et al., 2013; Llorens-Bobadilla et al., 2015; Mich et al., 2014). The majority of adult NSCs are produced during embryonic days (E13.5 - E15.5) in the mouse and remain largely quiescent until they become reactivated postnatally contributing to neurogenesis (Fuentealba et al., 2015; Furutachi et al., 2015).

Defects of neurogenesis occur during aging and most studies agree that it is related to a progressive reduction in the number of proliferating cells in the V-SVZ (Blackmore et al., 2009; Enwere et al., 2004; Maslov et al., 2004; Tropepe et al., 1997). Cell cycle alterations of NSCs or decline in their number explained the age-related neurogenesis decline and are already visible at 6 months in the adult mouse (Bouab et al., 2011; Daynac et al., 2016a; Daynac et al., 2014; Luo et al., 2008). Several factors from the neurogenic niche, including inflammatory factors, have been shown to reduce neurogenesis during aging by altering the cell cycle of NSCs (Daynac et al., 2014; Kalamakis et al., 2019; Pineda et al., 2013; Silva-Vargas et al., 2016). Quiescence of NSCs has also been shown to be triggered by Wnt antagonist in the aging brain (Kalamakis et al., 2019).

Syndecan-1 (SDC1, CD138) is a cell surface heparan sulfate proteoglycan that has been reported to modulate neural progenitor proliferation during embryogenesis through Wnt signaling pathways (Wang et al., 2012). Recently, we reported on a different expression

pattern of SDC1 between qNSCs and aNSCs and demonstrated its role in the proliferation of aNSCs in the postnatal V-SVZ (Morizur et al., 2018).

Here, we examined in more details alterations during aging of NSC proliferation from postnatal V-SVZ in mice particularly with regards to capacity of qNSCs to enter cell cycle and the effects of exogenous SDC1 on NSC proliferation.

Results

LeX^{bright} quiescent NSCs are produced during embryogenesis

We previously reported on a FACS strategy to sort LeX^{bright} qNSCs and LeX+EGFR+ aNSCs from the adult mouse and early postnatal V-SVZ based on the absence of CD24 expression and the differential expression of the membrane markers EGFR and LeX (Daynac et al., 2013; Daynac et al., 2015; Morizur et al., 2018). These LeX^{bright} qNSCs and LeX+EGFR+ aNSCs exhibit strinkingly similar molecular profiles to that obtained by other strategies, including anti-GLAST antibody, and/or transgenic GFAP::GFP mice in adult V-SVZ (Beckervordersandforth et al., 2010; Codega et al., 2014; Llorens-Bobadilla et al., 2015; Mich et al., 2014).

Adult NSCs have been reported to be produced during mid-embryonic development in the mouse and remain largely quiescent until they become reactivated postnatally (Fuentealba et al., 2015; Furutachi et al., 2015). Therefore, to mark qNSCs generated during embryogenesis, BrdU was administrated to pregnant mice from E14.5 to E15.5. qNSCs that underwent rare divisions, if any, were characterized by BrdU-label retention in postnatal brains (one month after birth). Immunostaining of SOX2 was used to confirm NSC identity and labeling of the G1-phase cell cycle marker MCM2 was used to detect both slowly and rapidly cycling NSCs (Maslov et al., 2004). LeX^{bright} qNSCs and LeX+EGFR+ aNSCs were sorted from V-SVZ one month after birth. Although they are actively dividing cells *in vivo* (Morizur et al., 2018), LeX+EGFR+ aNSCs were in great majority (72%) BrdU/SOX2/MCM2-triple positive and had a BrdU staining less intense in comparision to LeX^{bright} qNSCs suggesting that they derived from the later with few divisions (Figure 1 and Figure S1). On the other hand, the majority of LeX^{bright} cells (82%) was positive for BrdU confirming their embryonic origin (Figure 1 and Figure S1). Moreover, 56.8% of LeX^{bright} cells were BrdU/SOX2/MCM2-triple positive cells, *i.e.* very long term qNSCs, whereas 25% were BrdU+/SOX2+/MCM2-negative *i.e.* likely differentiated astrocytes.

These data confirmed thus that the LeX^{bright} qNSCs from the postnatal brain are produced during embryogenesis similarly as previously reported by others using *in vivo* approaches (Fuentealba et al., 2015; Furutachi et al., 2015).

The subpopulation of primed LeX^{bright} qNSCs able to enter the cell cycle rapidly decreases with age

Many structural and cellular modifications of the V-SVZ progressively occur during the early postnatal development and later in the adult brain, but data on the cell cycle status of NSCs associated with these changes are still incompletly documented. qNSCs and aNSCs identity in early postnatal V-SVZ was confirmed with GFAP expression, a marker of adult type B/NSCs (Doetsch et al.), and MCM2 expression. LeX^{bright} and LeX+EGFR+ cells were sorted from early postnatal V-SVZ (10 days). Both LeX^{bright} qNSCs and LeX+EGFR+ aNSCs expressed GFAP (Figure S2). MCM2, which is expressed in actively dividing cells and slowly cycling NSCs (Maslov et al., 2004), was detected on 65% of LeX+EGFR+ aNSCs but also 25% of LeX^{bright} qNSCs (Figure S2C), confirming that a part of qNSCs were primed to enter cell cycle at this developmental stage.

To further examine cell cycle alterations of NSC populations from early postnatal pups to aged mice, we used fluorescence ubiquitination cell cycle indicator (FUCCI) Cdt1-red transgenic mice. FUCCI-Cdt1 system allows the visualization of cells in G1 with the presence of a G1 specific red-Cdt1 reporter (FUCCI^{pos}), while it is absent in cells during the S/G2/M phases (FUCCI^{neg}) (Sakaue-Sawano et al., 2008). In addition, FUCCI^{high} allows the identification of cells that have exited the cell cycle (G0 cells) (Daynac et al., 2014; Roccio et al., 2013).

At each developmental stage, most LeX+EGFR+ aNSCs were in G1 (FUCCI^{low}) and in S/G2/M phases (FUCCI^{neg}) and fewer had exited cell cycle (FUCCI^{high}) accordingly to their active proliferating status (Figure 2A and Table S1). Interestingly, we found higher proportions of aNSCs in G0 (FUCCI^{high}) in the early postnatal brains as compared to the adult brains, which is reminiscent of an extensive differentiation associated with the brain development after birth. Moreover, the ratio of cells in G1 (FUCCI^{low}) over S/G2/M phases (FUCCI^{neg}) was higher in the early postnatal as compared to adult indicating a longer G1 phase.

On the contrary, a large proportion of LeX^{bright} qNSCs had exited the cell cycle (FUCCI^{high}) at all developmental stages in accordance with their quiescent status (Figure 2B). Nonetheless,

we found between 21.6 % and 33.2 % of LeX^{bright} qNSCs that were either in G1 (FUCCI^{low}) or in S/G2/M (FUCCI^{neg}), whatever the developmental stage, highlighting that a significant and stable fraction of qNSCs are primed to enter cell cycle in the V-SVZ from both early postnatal and adult mouse brain. Nonetheless, a significant fraction of LeX^{bright} qNSCs were in G1 (FUCCI^{low}) but few of them were actively cycling (FUCCI^{neg})(Figure 2B). Markedly, the percentage of LeX^{bright} qNSCs in S/G2/M (FUCCI^{neg}) dropped in the young adult mice (Figure 2B).

We then compared the capacities of LeX^{bright} qNSCs and LeX+EGFR+ aNSCs sorted from PN10 and young adult V-SVZ to proliferate and to form neurospheres, which are floating clones initiated by actively dividing NSCs (Pastrana et al., 2011). LeX+EGFR+ aNSCs had a similar clonogenic capacity in early postnatal and adult brains (Figure 2C). In addition, LeX+EGFR+ subpopulations were sorted according to FUCCI (FUCCI^{low}: G1 and FUCCI^{neg}: S/G2/M) but presented no difference of clonogenic capacity at both ages (Figure S3). Besides, accordingly with their quiescent status, LeX^{bright} qNSCs from neonatal brain had a 15.5 times lower clonogenic capacity than their activated LeX+EGFR+ aNSCs counterparts (Figure 2C). Clonogenic capacity of LeX^{bright} qNSCs was further decreased by more than 100-fold in the adult brain. This decrease in clonogenic capacity appeared to reflect the disappearing of clonogenic LeX^{brigh} cells rather than their positionning within cell cycle since LeX^{bright} FUCCI^{low} and FUCCI^{neg} had similar clonogenicity (Figure S3). This extremely low clonogenic capacity of LeX^{bright} qNSCs in youg adult V-SVZ contrasted with their MCM2 expression (Figure 1) suggesting that most primed LeX^{bright} qNSCs are not fully activated to generate clones.

Our data revealed an early cell cycle alteration of LeX+EGFR+ aNSCs in early postnatal pups most probably coinciding with differentiation during development. Additionnaly, some LeX^{bright} qNSCs entered the cell cycle in the early postnatal whereas they were blocked in G1 in the young adult mice.

A subpopulation of LeX^{bright} FUCCI$^{neg/low}$ qNSCs maintains the capacity to enter proliferation in the young adult V-SVZ

LeX^{bright} qNSC and LeX+EGFR+ aNSC populations were sorted from the V-SVZ of young adult mice then plated in enriched NSC medium supplemented with BrdU (10 µM) to challenge their proliferation capacities. After 72h, the great majority of LeX+EGFR+ aNSCs (84.2 ± 3.4%) had incorporated BrdU and exhibited an active protein synthesis activity as

seen with phosphorylation of S6 ribosomal protein (69.8 ± 3.4%)(Figure 3A-B). By contrast, only 27.2 ± 9.8% of LeX^{bright} qNSCs had incorprated BrdU and few of them (3.1 ± 1.6%) were positive for phosphoS6 ribosomal protein (Figure 3A-B). Both BrdU incorporation and pS6 suggested that a subpopulation of qNSCs was primed to enter cell cycle as previously reported (Codega et al., 2014; Llorens-Bobadilla et al., 2015).

To further explore the capacity of these LeX^{bright} qNSCs to re-enter into the cell cyle, we prospectively sorted them from the young adult FUCCI V-SVZ and challenged their proliferation capacities by *in vitro* timelaps videomicroscopy.

On one hand, FUCCI^{high} cells representing the majority of LeX^{bright} population (interquartile range [67.9%-79.2%]) had apparently exited the cell cycle and presented a bright red fluorescence *in vitro,* which eventually disappeared when cells died but they never divided (Figure 3C). On the other hand, 20% of the FUCCI$^{neg/low}$ population of LeX^{bright} qNSCs, encompassing G1 and scarce S/G2/M cells, had divided during the first 26h (Figure 3D). Then FUCCI fluorescence showed an increase which became high in some LeX^{bright} qNSCs. Thereafter, FUCCI$^{neg/low}$ LeX^{bright} qNSCs very scarcely generated clones that grew slowly and utimately gave rise to larger clones (Figure 3E).

Altogether these data show that some of the LeX^{bright} qNSCs were primed to re-enter cell cycle *in vitro* and were contained within the FUCCI$^{neg/low}$ population.

Recombinant Syndecan-1 shortens cell cycle progression *in vitro*

We have shown that SDC1 is highly expressed in proliferating LeX+EGFR+ aNSCs from adult mice while it is found at low levels in LeX^{bright} qNSCs (Morizur et al., 2018). Here, we reported that SDC1 mRNAs were expressed at a similar level in LeX+EGFR+ aNSCs from neonatal and adult mice (Figure S4). Although the expression of SDC1 mRNAs was low in LeX^{bright} qNSCs from neonates, it showed a further decline in adult mice (Figure S4) coinciding with the drop in clonogenic capacities. We have previously reported that SDC1 knockdown reduces proliferation of LeX+EGFR+ aNSCs (Morizur et al., 2018). Likewise, addition of Chondroitinase ABC (50 and 100 U/mL) which degrades chondroitin sulfate proteoglycans, including SDC1, reduced the formation of neurospheres initiated by LeX+EGFR+ aNSCs (data not shown). Conversely, deglycanation of SDC1 with Heparanase (4 ng/mL) which transforms SDC1 into a highly selective surface-binding protein (Ma et al., 2006) increased BrdU incorporation in proliferating NSCs (data not shown).

Therefore, we tested the effects of exogenous recombinant SDC1 (recSDC1) on proliferation of NSCs freshly sorted from young adult mice. Two days after plating, LeX+EGFR+ aNSCs gave rise to small colonies containing 4-6 cells in control conditions and 4-8 cells in the presence of 2.5µg/ml of recSDC1. This increase was further observed on neurosphere size at 6 days in the presence of 2.5 µg/ml of rec SDC1 (Figure 4A). This increase in neurosphere size inversely mirrored the data we previously reported after silencing SDC1 (Morizur et al., 2018). Besides, the clonogenic efficacy of LeX+EGFR+ aNSCs appeared to be almost significantly increased in the presence of recSDC1 (Figure 4B).

We thus investigated the effects of recSDC1on cell cycle length of LeX+EGFR+ aNSCs by timelapse videomicroscopy using FUCCI mice. Interestingly, the time for the first division of LeX+EGFR+ aNSCs from neonates was significantly shortened in the presence of 2.5µg/ml of recSDC1 in comparison to control (Figure 4C). A similar shorthening was observed in young adult V-SVZ (Figure S5). The length of the G1 phase was measured for the subsequent cycle taking advantage of the FUCCI Cdt1 fluorescence. A significant shorthening of the G1 phase was observed in LeX+EGFR+ aNSCs (Figure 4D). We then investigated the effects of recSDC1 on LeX^{bright} $FUCCI^{neg/low}$ qNSCs, *i.e.* primed qNSCs. The percentage of dividing LeX^{bright} $FUCCI^{neg/low}$ appeared not significantly increased in the presence of SDC1 (Figure 4E). Strikingly, the time for the first division of LeX^{bright} $FUCCI^{neg/low}$ qNSCs was significantly shortened in the presence of 2.5µg/ml of recSDC1 (7h36) in comparison to control (9h12) (Figure 4F). However, LeX^{bright} $FUCCI^{neg/low}$ cells remained FUCCI Cdt1 positive at the end of the videomicroscopy (28-30h) and did not reenter in another division cycle even in the presence of recSDC1. By contrast, $FUCCI^{high}$ LeX^{bright} cells did not divide even in the presence of SDC1 (data not shown). Strikingly, 25% (first interquartile) of LeX^{bright} $FUCCI^{neg/low}$ and LeX+EGFR+ NSCs exposed to SDC1 had divided before 5h and 7h for adults and neonates, respectively, suggesting that numerous aNSCs and qNSCs might be blocked in G_2.

Altogether, our data show that SDC1 favored cell cycle progression of primed qNSCs and aNSCs.

Recombinant Syndecan-1 accelerates recovery of neurogenic populations *in vivo*

Subsequently, we addressed the capacity of recSDC1 to ameliorate V-SVZ recovery *in vivo* after brain irradiation in young adult FUCCI-Cdt1 transgenic mice. After such radiation-

induced injury, highly proliferating cells, including LeX+EGFR+ aNSCs, are rapidly eliminated whereas LeX^{bright} qNSCs are radioresistant and enter cell cycle 48h after exposure, which is followed by the progressive recolonization of the V-SVZ by LeX+EGFR+ aNSCs, EGFR+ progenitors and CD24+EGFR+ young neuroblasts (Daynac et al., 2013). Collection of V-SVZ cells from young adult FUCCI Cdt1 mice 48h after irradiation demonstrated the elimination of the majority of LeX+EGFR+ aNSCs, EGFR+ and CD24+EGFR+ cells while leaving a significant amount of LeX^{bright} FUCCI$^{neg/low}$ qNSCs, *i.e.* progressing throughout the cell cycle (Figure 5). Recombinant SDC1 was administrated intraventricularly while mice received BrdU through systemic route and recovery of neurogenic populations was analyzed three days later. The absolute counts of the neurogenic populations revealed that recSDC1 favored primarily the recovery of EGFR+ and CD24+EGFR+ cells (Figure 5 and Figure S6A). Interestingly, the increase in these EGFR+ and CD24+EGFR+ neurogenic populations with recSDC1 was observed in the FUCCI^{low} and FUCCI^{neg} cycling populations (Figure 5C-D) and was associated with BrdU incorporation, *i.e*. proliferation (Figure S6B). On the other hand, the presence of recSDC1 did not significantly improve the recovery of LeX^{bright} qNSCs and LeX+EGFR+ aNSCs (Figure 5A-B) while BrdU incorporation indicated their proliferation (Figure S6B). Part of the LeX+EGFR+ aNSCs had even exited cell cycle, i.e. FUCCI^{high} (Figure 2B). Nevertheless, this would be expected from asymmetric division of NSCs and their subsequent loss instead of EGFR+ and CD24+EGFR+ which undergo symmetric division.

These data show that SDC1 favored recovery of neurogenic populations in the V-SVZ after injury.

Discussion

Different FACS strategies have been reported for the isolation of qNSCs and aNSCs (Beckervordersandforth et al., 2010; Codega et al., 2014; Daynac et al., 2013; Llorens-Bobadilla et al., 2015; Mich et al., 2014). Briefly, anti-GLAST or anti-LeX antibodies or GFAP::GFP are used as NSC markers in combination with other markers. Interestingly, qNSCs and aNSCs obtained from these different methods have strikingly similar molecular profiles. Particularly, qNSCs being characterized by the expression of several genes as Prom1, Aldh1l1, Gjb6, CD9, Sox9, Id2 and Id3 whereas aNSCs expressing high level of Ascl1, Egr1, Fos, Sox4 and Sox11 (Beckervordersandforth et al., 2010; Codega et al., 2014; Daynac et al., 2013; Llorens-Bobadilla et al., 2015; Mich et al., 2014). In addition, we have shown that

LeX^{bright} qNSCs are produced during embryogenesis similarly as previously reported by for type B/NSCs *in vivo* (Fuentealba et al., 2015; Furutachi et al., 2015).

A pool of NSCs remains largely dormant until qNSCs become reactivated postnatally contributing to neurogenesis for brain homeostasis or repair after injury (Daynac et al., 2013). Using the FUCCI-Cdt1 system, we reported, here, on the prospective isolation of primed qNSC. Interestingly, we demonstrate that the capacity of qNSCs to enter cell cycle declines as early as in the young adult mouse brain. However, we have shown that cell cycle progression of LeX^{bright} qNSCs is favored by addition of exogenous SDC1.

Adult neurogenesis declines with aging due to the depletion and functional impairment of neural stem/progenitor cells. In this context, previous reports have indicated that the number of NSCs in the mouse V-SVZ declines by mid-age (10-12 months), with an additional reduction in older mice (22 months) reviewed in (Lupo et al., 2019). While prior studies have demonstrated a reduction of NSC content and have noted a paradoxical increase in the NSC division rate in old animals (Luo et al., 2008; Shook et al., 2012), we observed a decline in cell cycle activity of aNSCs at mid-age (6-12 months) but with stable contents (Daynac et al., 2016a; Daynac et al., 2014). These seemingly divergent data are reconciled by the fluctuation of NSC proliferation with a decline bewteen 2 and 18 months, then unexpectedly a reversal faster cell cycle at 22 months (Apostolopoulou et al., 2017). On the other hand, increasing NSC quiescence are predicted to contribute to the age-related decline of neurogenesis (Bast et al., 2018; Kalamakis et al., 2019). NSCs begin undergoing quiescence-associated changes at mid-adulthood in the mouse V-SVZ (Bouab et al., 2011).

Using various approaches based on FUCCI-Cdt1, BrdU incorporation, clonogenicity, which showed consistency, we have shown that proliferation capacities of NSCs decreased early in the postnatal V-SVZ. Particularly, aNSCs showed a G1 lengthening in the early postnatal V-SVZ associated with cell cycle exit which is in accordance with differentiation during brain development (Salomoni and Calegari, 2010). Grippingly, we have identified a population among LeX^{bright} qNSCs that are characterized by a low FUCCI-Cdt1 fluorescence which are primed to enter the cell cycle. The population of LeX^{bright} is abble to re-entry into cell cycle after V-SVZ irradiation accordingly to what was previously reported (Daynac et al., 2013) and similarly to what was shown for other brain injuries (Codega et al., 2014; Llorens-Bobadilla et al., 2015; Mich et al., 2014). Noticeably, we have shown a drop of primed LeX^{bright} FUCCI^{neg} qNSCs entering the cell cycle in the young adult which was associated to the decline in their clonogenic capacities. Although expressing a significant level of SOX2

and MCM2, marking slow dividing NSC (Maslov et al., 2004), LeX^{bright} cells divided once, then stopped in G_1 but very scarcely formed neurospheres in neonates and even more rarely when isolated from young adults. This might indicate that experimental conditions are not adequate for NSC proliferation *in vitro* and/or that high LeX expression interferred with NSC proliferation as previously reported (Luque-Molina et al., 2017). These early events are reminiscent to the human V-SVZ which shows a drop in neurogenesis several months after birth (Sanai et al., 2011). This continuum of NSC proliferation decline starting at birth is linked to postnatal brain development. Also, this suggests that qNSCs are recruted, through their activation, early during the postnatal brain development. Therefore, NSC quiescence appears as a programmed developmental process and a consequence of molecular aging processes.

Loss of the ability of qNSCs to activate and/or proliferation defect during aging are related to alterations of transcriptomic or lysosomal activities (Leeman et al., 2018; Lupo et al., 2018). Raise in inflammatory factors within the neurogenic niche has also been shown to reduce neurogenesis by altering the cell cycle or quiescence of NSCs during aging (Daynac et al., 2016a; Daynac et al., 2014; Engler et al., 2018; Kalamakis et al., 2019; Pineda et al., 2013; Silva-Vargas et al., 2016). Several signaling pathways such as WNT or Sonic Hedgehog (SHH) have been involved in the regulation of NSC quiescence and proliferation (Chavali et al., 2018; Daynac et al., 2016b). Interestingly, activation of LeX^{bright} qNSCs after radio-induced injury was associated with the upregulation of several genes belonging to WNT signaling (Table S2). Conversely, the niche-derived WNT antagonist sFRP5 has been shown to induce quiescence in the aging brain (Kalamakis et al., 2019).

SDC1 plays a role in NSC proliferation during embryogenesis and in postnatal NSCs (Morizur et al., 2018; Wang et al., 2012). SDC1 regulates proliferation in part by modulating the ability of neural progenitors to respond to WNT ligands (Wang et al., 2012). Here, we have shown that addition of exogenous SDC1 favors proliferation of aNSCs *in vitro* through the reduction of the G1 phase. Morever, exogenous SDC1 hastened the time for the first division of primed qNSCs. Interestingly, numerous NSCs divided early after exogenous SDC1 treatment suggesting that they are paused in G_2, as reported in the drosophila (Otsuki and Brand, 2018). Whether these proliferation effects involved WNT signaling needs to be further investigated. Grippingly, exogenous SDC1 also demonstrated *in vivo* activity by favoring recovery of neurogenic populations after V-SVZ injury. Therefore, SDC1 might be used to counteract brain injury. If validated in older animals, administration of SDC1, or of an

agonist, might provide the means to control the proliferation of NSCs and to counteract the neurogenesis decline during aging which is still a major concern.

Limitations of the study

This study has some limitations that should be kept in mind when interpreting the relevance of the findings to regeneration of neurons. Primed LeX^{bright} qNSCs were able to make only a single division suggesting that unknown factor(s) are further required to insure subsequent divisions. Nevertheless, molecular characterization of this rare population might be helpful to identify such factor(s). The administration of recombinant Syndecan-1 ameliorated the recovery of neurogenic populations *in vivo* but the target cells have to be further characterized. In addition, the production of neurons and their fonctionality remain to be analysed. Finally, the transfer to clinic has to take into accout that Syndecan-1 might be hijacked by cancer cells to proliferate.

Resource Availability

Lead Contact

Further requests should be directed to and will be fulfilled by the Lead Contact: Marc-André Mouthon (marc-andre.mouthon@cea.fr).

Materials Availability

The study did not generate any unique reagent.

Data and Code Availability

This published article includes all datasets generated or analyzed during this study.

Acknowledgements

We are indebted to S. Vincent-Naulleau, V. Neuville, V. Barroca, S. Devanand and the staff of the animal facilities; to V. Mesnard for irradiation; to J. Baijer and N. Dechamps for cell sorting; and to A. Gouret and A. Leliard for their precious administrative assistance. Flow cytometry and cell sorting were performed at the iRCM Flow Cytometry Shared Resource, established by equipment grants from DIM-Stem-Pôle, INSERM, Foundation ARC, and CEA. This work was supported by grants from Electricité de France (EDF) and CEA (Segment Radiobiologie).

Transparent Methods

All methods can be found in the accompanying Transparent Methods supplemental file.

Author Contributions

M.A.M: conception and supervision, collection and/or assembly of data, data analysis, interpretation and manuscript writing. L.M: conception and design, collection and/or assembly of data, data analysis, interpretation and manuscript writing. L.D., D.P., T.K.: collection and/or assembly of data. F.D.B: funding acquisition, conception, supervision and manuscript writing.

Declaration of Interests

The authors declare no conflict of interest.

References

Apostolopoulou, M., Kiehl, T. R., Winter, M., Cardenas De La Hoz, E., Boles, N. C., Bjornsson, C. S., Zuloaga, K. L., Goderie, S. K., Wang, Y., Cohen, A. R., and Temple, S. (2017). Non-monotonic Changes in Progenitor Cell Behavior and Gene Expression during Aging of the Adult V-SVZ Neural Stem Cell Niche. Stem Cell Reports *9*, 1931-1947.

Bast, L., Calzolari, F., Strasser, M. K., Hasenauer, J., Theis, F. J., Ninkovic, J., and Marr, C. (2018). Increasing Neural Stem Cell Division Asymmetry and Quiescence Are Predicted to Contribute to the Age-Related Decline in Neurogenesis. Cell Rep *25*, 3231-3240 e3238.

Beckervordersandforth, R., Tripathi, P., Ninkovic, J., Bayam, E., Lepier, A., Stempfhuber, B., Kirchhoff, F., Hirrlinger, J., Haslinger, A., Lie, D. C., *et al.* (2010). In vivo fate mapping and expression analysis reveals molecular hallmarks of prospectively isolated adult neural stem cells. Cell Stem Cell *7*, 744-758.

Blackmore, D. G., Golmohammadi, M. G., Large, B., Waters, M. J., and Rietze, R. L. (2009). Exercise increases neural stem cell number in a growth hormone-dependent manner, augmenting the regenerative response in aged mice. Stem Cells *27*, 2044-2052.

Bouab, M., Paliouras, G. N., Aumont, A., Forest-Berard, K., and Fernandes, K. J. (2011). Aging of the subventricular zone neural stem cell niche: evidence for quiescence-associated changes between early and mid-adulthood. Neuroscience *173*, 135-149.

Chavali, M., Klingener, M., Kokkosis, A. G., Garkun, Y., Felong, S., Maffei, A., and Aguirre, A. (2018). Non-canonical Wnt signaling regulates neural stem cell quiescence during homeostasis and after demyelination. Nat Commun *9*, 36.

Codega, P., Silva-Vargas, V., Paul, A., Maldonado-Soto, A. R., Deleo, A. M., Pastrana, E., and Doetsch, F. (2014). Prospective identification and purification of quiescent adult neural stem cells from their in vivo niche. Neuron *82*, 545-559.

Daynac, M., Chicheportiche, A., Pineda, J. R., Gauthier, L. R., Boussin, F. D., and Mouthon, M. A. (2013). Quiescent neural stem cells exit dormancy upon alteration of GABAAR signaling following radiation damage. Stem Cell Res *11*, 516-528.

Daynac, M., Morizur, L., Chicheportiche, A., Mouthon, M. A., and Boussin, F. D. (2016a). Age-related neurogenesis decline in the subventricular zone is associated with specific cell cycle regulation changes in activated neural stem cells. Sci Rep *6*, 21505.

Daynac, M., Morizur, L., Kortulewski, T., Gauthier, L. R., Ruat, M., Mouthon, M. A., and Boussin, F. D. (2015). Cell Sorting of Neural Stem and Progenitor Cells from the Adult Mouse Subventricular Zone and Live-imaging of their Cell Cycle Dynamics. J Vis Exp.

Daynac, M., Pineda, J. R., Chicheportiche, A., Gauthier, L. R., Morizur, L., Boussin, F. D., and Mouthon, M. A. (2014). TGFbeta lengthens the G1 phase of stem cells in aged mouse brain. Stem Cells *32*, 3257-3265.

Daynac, M., Tirou, L., Faure, H., Mouthon, M. A., Gauthier, L. R., Hahn, H., Boussin, F. D., and Ruat, M. (2016b). Hedgehog Controls Quiescence and Activation of Neural Stem Cells in the Adult Ventricular-Subventricular Zone. Stem Cell Reports *7*, 735-748.

Doetsch, F., Caille, I., Lim, D. A., Garcia-Verdugo, J. M., and Alvarez-Buylla, A. (1999). Subventricular zone astrocytes are neural stem cells in the adult mammalian brain. Cell *97*, 703-716.

Engler, A., Rolando, C., Giachino, C., Saotome, I., Erni, A., Brien, C., Zhang, R., Zimber-Strobl, U., Radtke, F., Artavanis-Tsakonas, S.*, et al.* (2018). Notch2 Signaling Maintains NSC Quiescence in the Murine Ventricular-Subventricular Zone. Cell Rep *22*, 992-1002.

Enwere, E., Shingo, T., Gregg, C., Fujikawa, H., Ohta, S., and Weiss, S. (2004). Aging results in reduced epidermal growth factor receptor signaling, diminished olfactory neurogenesis, and deficits in fine olfactory discrimination. J Neurosci *24*, 8354-8365.

Fuentealba, L. C., Rompani, S. B., Parraguez, J. I., Obernier, K., Romero, R., Cepko, C. L., and Alvarez-Buylla, A. (2015). Embryonic Origin of Postnatal Neural Stem Cells. Cell *161*, 1644-1655.

Furutachi, S., Miya, H., Watanabe, T., Kawai, H., Yamasaki, N., Harada, Y., Imayoshi, I., Nelson, M., Nakayama, K. I., Hirabayashi, Y., and Gotoh, Y. (2015). Slowly dividing neural progenitors are an embryonic origin of adult neural stem cells. Nat Neurosci *18*, 657-665.

Kalamakis, G., Brune, D., Ravichandran, S., Bolz, J., Fan, W., Ziebell, F., Stiehl, T., Catala-Martinez, F., Kupke, J., Zhao, S.*, et al.* (2019). Quiescence Modulates Stem Cell Maintenance and Regenerative Capacity in the Aging Brain. Cell *176*, 1407-1419 e1414.

Kempermann, G., Gage, F. H., Aigner, L., Song, H., Curtis, M. A., Thuret, S., Kuhn, H. G., Jessberger, S., Frankland, P. W., Cameron, H. A.*, et al.* (2018). Human Adult Neurogenesis: Evidence and Remaining Questions. Cell Stem Cell *23*, 25-30.

Leeman, D. S., Hebestreit, K., Ruetz, T., Webb, A. E., McKay, A., Pollina, E. A., Dulken, B. W., Zhao, X., Yeo, R. W., Ho, T. T.*, et al.* (2018). Lysosome activation clears aggregates and enhances quiescent neural stem cell activation during aging. Science *359*, 1277-1283.

Llorens-Bobadilla, E., Zhao, S., Baser, A., Saiz-Castro, G., Zwadlo, K., and Martin-Villalba, A. (2015). Single-Cell Transcriptomics Reveals a Population of Dormant Neural Stem Cells that Become Activated upon Brain Injury. Cell Stem Cell *17*, 329-340.

Luo, J., Shook, B. A., Daniels, S. B., and Conover, J. C. (2008). Subventricular zone-mediated ependyma repair in the adult mammalian brain. J Neurosci *28*, 3804-3813.

Lupo, G., Gioia, R., Nisi, P. S., Biagioni, S., and Cacci, E. (2019). Molecular Mechanisms of Neurogenic Aging in the Adult Mouse Subventricular Zone. J Exp Neurosci *13*, 1179069519829040.

Lupo, G., Nisi, P. S., Esteve, P., Paul, Y. L., Novo, C. L., Sidders, B., Khan, M. A., Biagioni, S., Liu, H. K., Bovolenta, P.*, et al.* (2018). Molecular profiling of aged neural progenitors identifies Dbx2 as a candidate regulator of age-associated neurogenic decline. Aging Cell *17*, e12745.

Luque-Molina, I., Khatri, P., Schmidt-Edelkraut, U., Simeonova, I. K., Holzl-Wenig, G., Mandl, C., and Ciccolini, F. (2017). Bone Morphogenetic Protein Promotes Lewis X Stage-Specific Embryonic Antigen 1 Expression Thereby Interfering with Neural Precursor and Stem Cell Proliferation. Stem Cells *35*, 2417-2429.

Ma, P., Beck, S. L., Raab, R. W., McKown, R. L., Coffman, G. L., Utani, A., Chirico, W. J., Rapraeger, A. C., and Laurie, G. W. (2006). Heparanase deglycanation of syndecan-1 is required for binding of the epithelial-restricted prosecretory mitogen lacritin. J Cell Biol *174*, 1097-1106.

Maslov, A. Y., Barone, T. A., Plunkett, R. J., and Pruitt, S. C. (2004). Neural stem cell detection, characterization, and age-related changes in the subventricular zone of mice. J Neurosci *24*, 1726-1733.

Mich, J. K., Signer, R. A., Nakada, D., Pineda, A., Burgess, R. J., Vue, T. Y., Johnson, J. E., and Morrison, S. J. (2014). Prospective identification of functionally distinct stem cells and neurosphere-initiating cells in adult mouse forebrain. Elife *3*, e02669.

Morizur, L., Chicheportiche, A., Gauthier, L. R., Daynac, M., Boussin, F. D., and Mouthon, M. A. (2018). Distinct Molecular Signatures of Quiescent and Activated Adult Neural Stem Cells Reveal Specific Interactions with Their Microenvironment. Stem Cell Reports *11*, 565-577.

Obernier, K., and Alvarez-Buylla, A. (2019). Neural stem cells: origin, heterogeneity and regulation in the adult mammalian brain. Development *146*.

Otsuki, L., and Brand, A. H. (2018). Cell cycle heterogeneity directs the timing of neural stem cell activation from quiescence. Science *360*, 99-102.

Pastrana, E., Silva-Vargas, V., and Doetsch, F. (2011). Eyes wide open: a critical review of sphere-formation as an assay for stem cells. Cell Stem Cell *8*, 486-498.

Pineda, J. R., Daynac, M., Chicheportiche, A., Cebrian-Silla, A., Sii Felice, K., Garcia-Verdugo, J. M., Boussin, F. D., and Mouthon, M. A. (2013). Vascular-derived TGF-beta increases in the stem cell niche and perturbs neurogenesis during aging and following irradiation in the adult mouse brain. EMBO Mol Med *5*, 548-562.

Roccio, M., Schmitter, D., Knobloch, M., Okawa, Y., Sage, D., and Lutolf, M. P. (2013). Predicting stem cell fate changes by differential cell cycle progression patterns. Development *140*, 459-470.

Sakaue-Sawano, A., Kurokawa, H., Morimura, T., Hanyu, A., Hama, H., Osawa, H., Kashiwagi, S., Fukami, K., Miyata, T., Miyoshi, H., *et al.* (2008). Visualizing spatiotemporal dynamics of multicellular cell-cycle progression. Cell *132*, 487-498.

Salomoni, P., and Calegari, F. (2010). Cell cycle control of mammalian neural stem cells: putting a speed limit on G1. Trends Cell Biol *20*, 233-243.

Sanai, N., Nguyen, T., Ihrie, R. A., Mirzadeh, Z., Tsai, H. H., Wong, M., Gupta, N., Berger, M. S., Huang, E., Garcia-Verdugo, J. M., *et al.* (2011). Corridors of migrating neurons in the human brain and their decline during infancy. Nature *478*, 382-386.

Shook, B. A., Manz, D. H., Peters, J. J., Kang, S., and Conover, J. C. (2012). Spatiotemporal changes to the subventricular zone stem cell pool through aging. J Neurosci *32*, 6947-6956.

Silva-Vargas, V., Maldonado-Soto, A. R., Mizrak, D., Codega, P., and Doetsch, F. (2016). Age-Dependent Niche Signals from the Choroid Plexus Regulate Adult Neural Stem Cells. Cell Stem Cell *19*, 643-652.

Tropepe, V., Craig, C. G., Morshead, C. M., and van der Kooy, D. (1997). Transforming growth factor-alpha null and senescent mice show decreased neural progenitor cell proliferation in the forebrain subependyma. J Neurosci *17*, 7850-7859.

Wang, Q., Yang, L., Alexander, C., and Temple, S. (2012). The niche factor syndecan-1 regulates the maintenance and proliferation of neural progenitor cells during mammalian cortical development. PLoS One *7*, e42883.

Figure 1: Young adult LeX^{bright} qNSCs are produced during embryogenesis. See also Figure S1.

BrdU was given to pregnant mice (from E14.5 to E15.5), then LeX+EGFR+ aNSCs and LeX^{bright} qNSCs were sorted using a combination of CD24/LeX/EGFR membrane markers one month after birth and BrdU incorporation was quantified together with SOX2 and MCM2. Data are represented as median ± interquartile range from replicate experiments (n = 4) with 2 to 4 mice per group.

Figure 2: Cell cycle status and clonogenic capacities of LeX^{bright} qNSCs and LeX+EGFR+ aNSCs in the postnatal V-SVZ. See also Table S1 and Figure S3.

FUCCI fluorescence was determined by flow cytometry in V-SVZ at various postnatal ages. The percentage of different FUCCI populations (FUCCI^{high}: G0; FUCCI^{low}: G1 and FUCCI^{neg}: S/G2/M) was represented among (A) LeX+EGFR+ aNSCs and (B) LeX^{bright} qNSCs. (C) The formation of neurospheres, i.e. clonogenic capacity, was determined 7 days after sorting LeX^{bright} qNSCs and LeX+EGFR+ aNSCs from 10 days- and 2 months-old V-SVZ. Data were compared using non-parametric Kruskal-Wallis and Dunn's multicomparison tests and given in Table S1. Data are represented as median ± interquartile. Each dot in C represents individual experiment.

Figure 3: LeX^{bright} FUCCI$^{neg/low}$ qNSCs divide and initiate clones *in vitro* but FUCCI^{high} NSCs have definitively exited the cell cycle.

LeX^{bright} qNSCs and LeX+EGFR+ aNSCs were sorted from young adult mouse V-SVZ, then cultured in the presence of BrdU for 72h in vitro. (A) Percentages of BrdU incorporation and (B) pS6-positive cells were quantified in LeX^{bright} qNSCs and LeX+EGFR+ aNSCs from replicate experiments with a total number of 66 to 144 cells. (C-E) LeX^{bright} cells were sorted from young adult V-SVZ according to their FUCCI-Cdt1 fluorescence intensity and were followed by time-lapse videomicroscopy. (C) LeX^{bright} FUCCI^{high} cells never divide but (D) the LeX^{bright} FUCCI$^{neg/low}$ population showed divisions. (E) Therafter, formation of clones was rarely observed in the LeX^{bright} FUCCI$^{neg/low}$ qNSCs. Scale bars = 10µm.

Figure 4: Recombinant SDC1 increases the neurosphere size of aNSCs and hastens the division of aNSCs and qNSCs. See also Figure S5.

(A-B) LeX+EGFR+ aNSCs were sorted from young adult V-SVZ. After 6 days in culture of LeX+EGFR+ aNSCs in the absence, or the presence, of 2.5µg/ml recSDC1: (A) the neurosphere area (µm²) and (B) clonogenic capacities were determined. (C-D) LeX+EGFR+ aNSCs were sorted from FUCCI neonates were followed by timelapse for 26-30h in the absence, or the presence, of 2.5µg/ml recSDC1, then (C) the time for the first division and (D) the length of the subsequent G_1 were recorded. (E-F) LeX^{bright} $FUCCI^{neg/low}$ qNSCs were sorted from adult FUCCI mice, then (E) the percentage of dividing cells/field and (F) the time for the first division were recorded. Data are represented as the median ± interquartile range of replicate experiments with 2to 4 mice per group.

Figure 5: Exogenous SDC1 favors recovery of neurogenic populations after radiation-induced V-SVZ injury. See also Figure S6.

Two-months-old adult FUCCI-Cdt1 mice were irradiated (4 Gy/head only) and received recSDC1 intraventricularly. The absolute numbers of (A) LeX^{bright} qNSCs, (B) LeX+EGFR+ aNSCs, (C) EGFR+ progenitors and (D) CD24+EGFR+ proliferating neuroblasts and FUCCI fluorescence were determined by flow cytometry within FUCCI subpopulations ($FUCCI^{high}$: G0; $FUCCI^{low}$: G1 and $FUCCI^{neg}$: S/G2/M). Data are represented as median ± interquartile range. Each plot represents an individual mouse (the number of mice is indicated within bars). Data were compared using non-parametric Kruskal-Wallis and Dunn's multicomparison tests. Comparisons with the Ctrl group are given upper the boxes and comparisons between PBS and recSDC1 over the brakets (° for $FUCCI^{high}$; # for $FUCCI^{low}$ and * for $FUCCI^{neg}$).

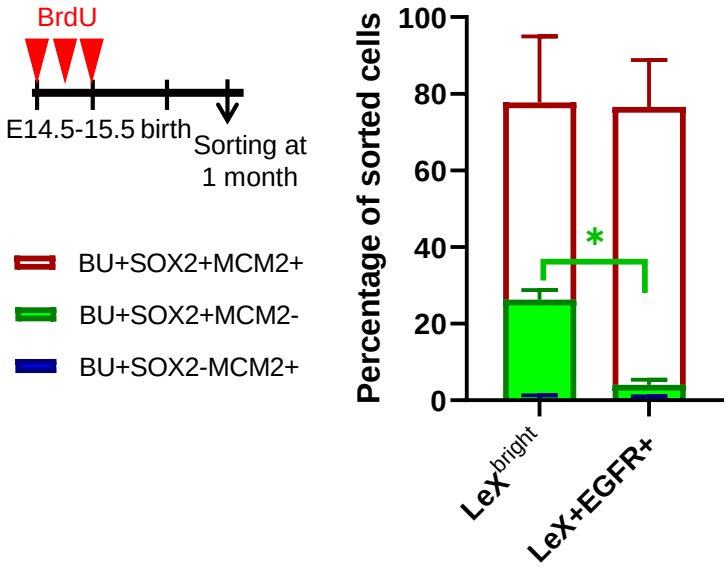
BrdU
E14.5-15.5 birth
Sorting at
1 month
BU+SOX2+MCM2+
BU+SOX2+MCM2-
BU+SOX2-MCM2+
Percentage of sorted cells
100
80
60
40
20
0
*
LeX^bright
LeX+EGFR+

Figure 1

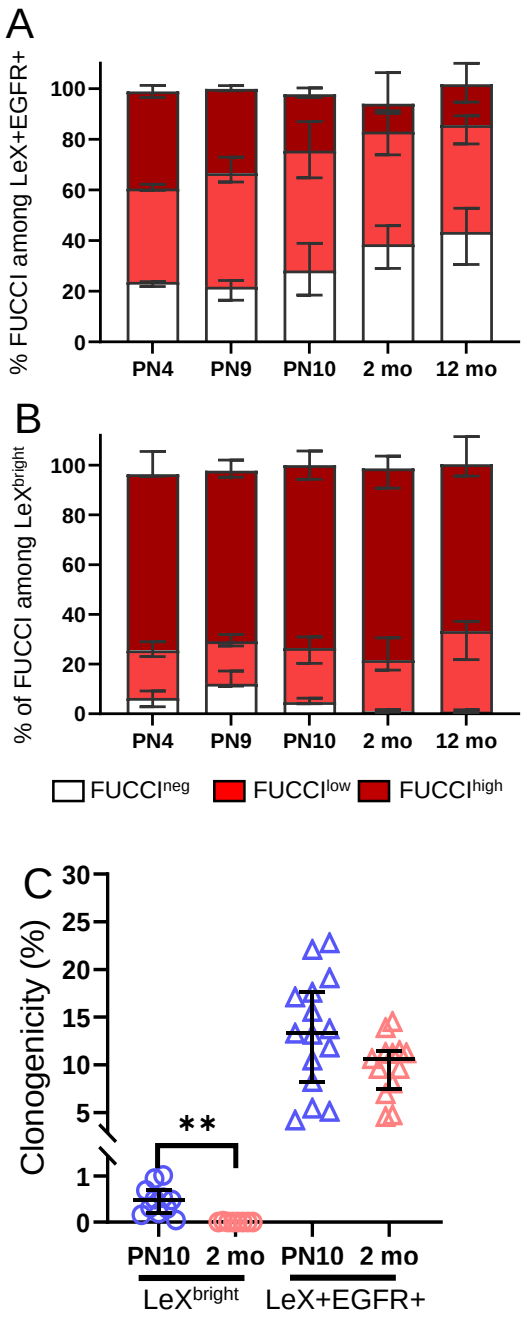
A
% FUCCI among LeX+EGFR+
100
80
60
40
20
0
PN4
PN9
PN10
2 mo
12 mo
B
% of FUCCI among LeXbright
100
80
60
40
20
0
PN4
PN9
PN10
2 mo
12 mo
FUCCIneg
FUCCIlow
FUCCIhigh
C
Clonogenicity (%)
30
25
20
15
10
5
1
0
**
PN10
2 mo
PN10
2 mo
LeXbright
LeX+EGFR+

Figure 2

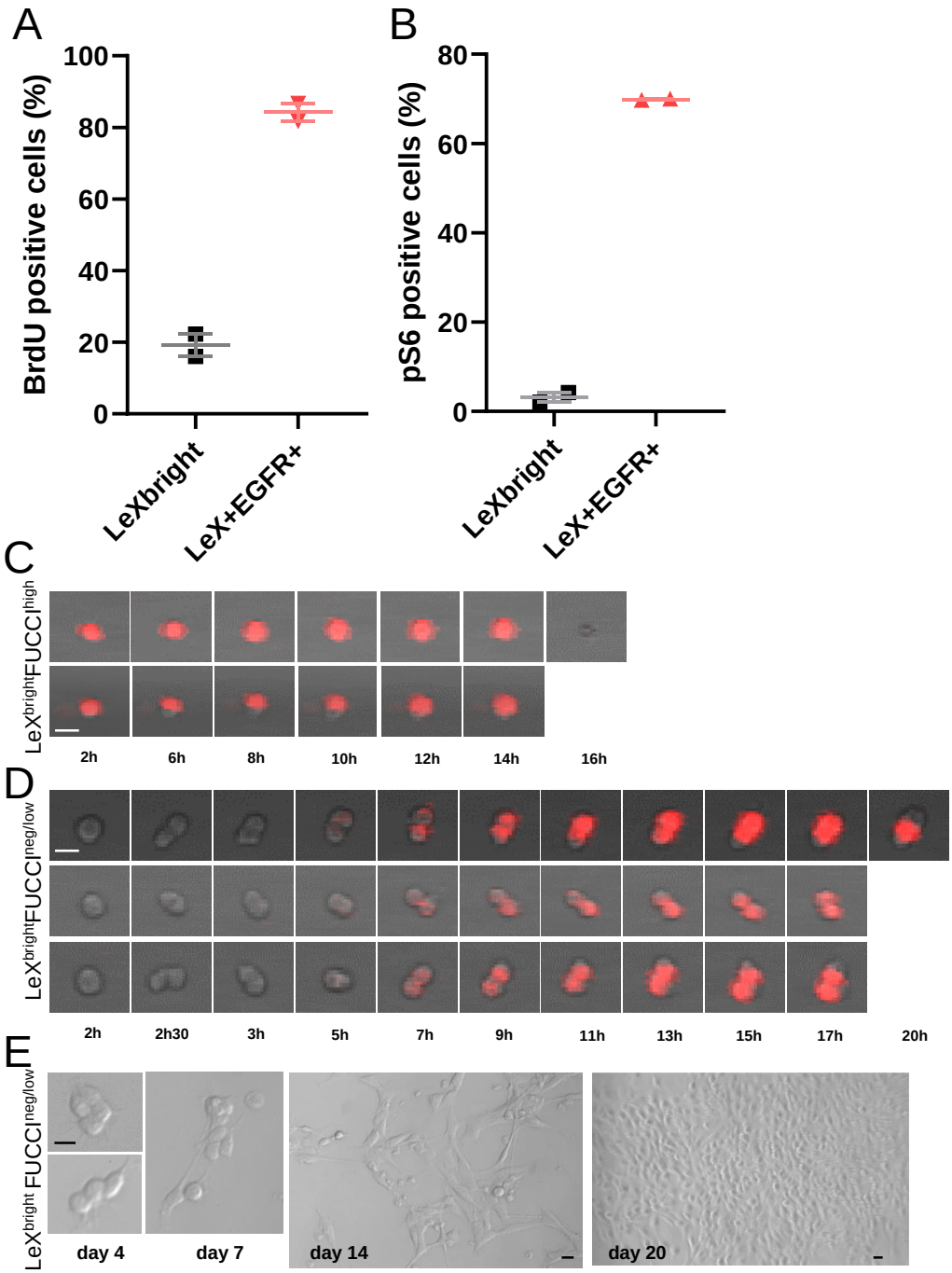
A
BrdU positive cells (%)
100
80
60
40
20
0
LeXbright
LeX+EGFR+
B
pS6 positive cells (%)
80
60
40
20
0
LeXbright
LeX+EGFR+
C
LeXbrightFUCCIhigh
2h
6h
8h
10h
12h
14h
16h
D
LeXbrightFUCCIneg/low
2h
2h30
3h
5h
7h
9h
11h
13h
15h
17h
20h
E
LeXbright FUCCIneg/low
day 4
day 7
day 14
day 20

Figure 3

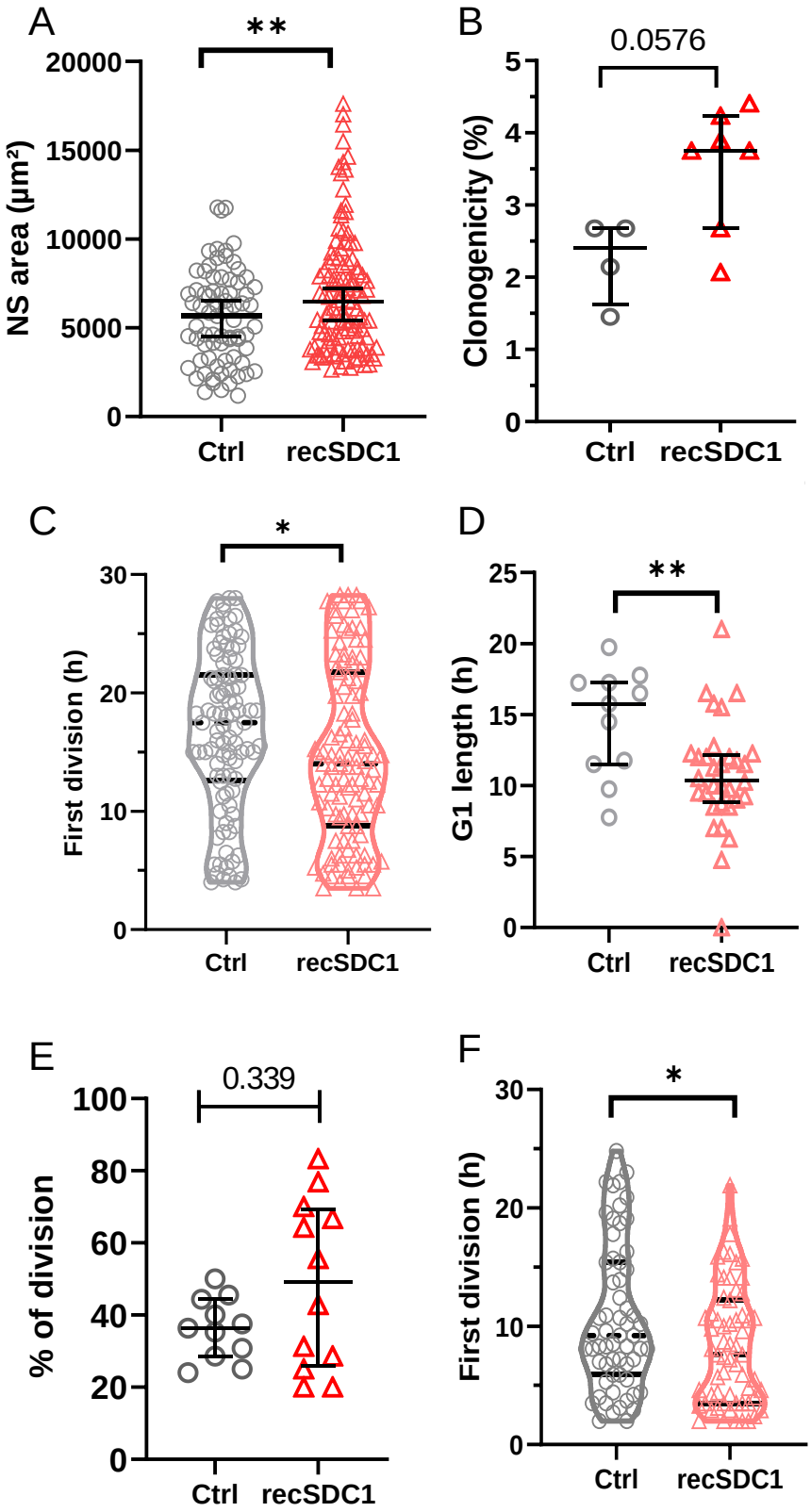
A
**
NS area (µm²)
20000
15000
10000
5000
0
Ctrl
recSDC1
B
0.0576
Clonogenicity (%)
5
4
3
2
1
0
Ctrl
recSDC1
C
*
First division (h)
30
20
10
0
Ctrl
recSDC1
D
**
G1 length (h)
25
20
15
10
5
0
Ctrl
recSDC1
E
0.339
% of division
100
80
60
40
20
0
Ctrl
recSDC1
F
*
First division (h)
30
20
10
0
Ctrl
recSDC1

Figure 4

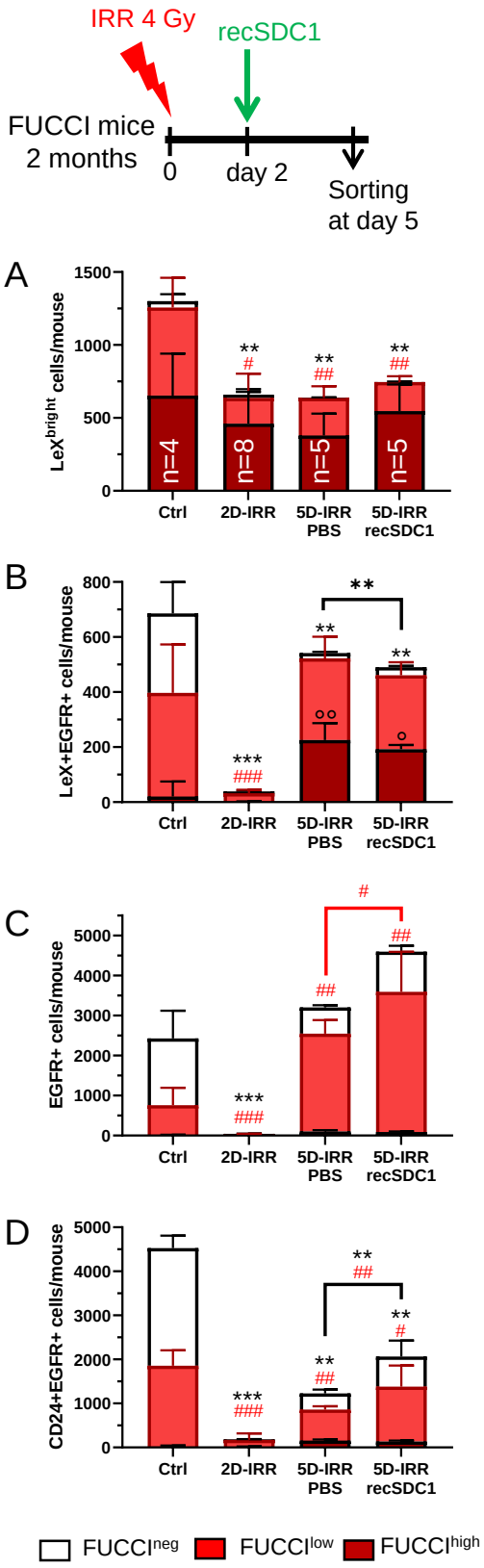
IRR 4 Gy
recSDC1
FUCCI mice
2 months
0
day 2
Sorting
at day 5
A
LeX^bright cells/mouse
1500
1000
500
0
n=4
n=8
n=5
n=5
Ctrl
2D-IRR
5D-IRR PBS
5D-IRR recSDC1
B
LeX+EGFR+ cells/mouse
800
600
400
200
0
C
EGFR+ cells/mouse
5000
4000
3000
2000
1000
0
D
CD24+EGFR+ cells/mouse
FUCCI^neg
FUCCI^low
FUCCI^high

Figure 5

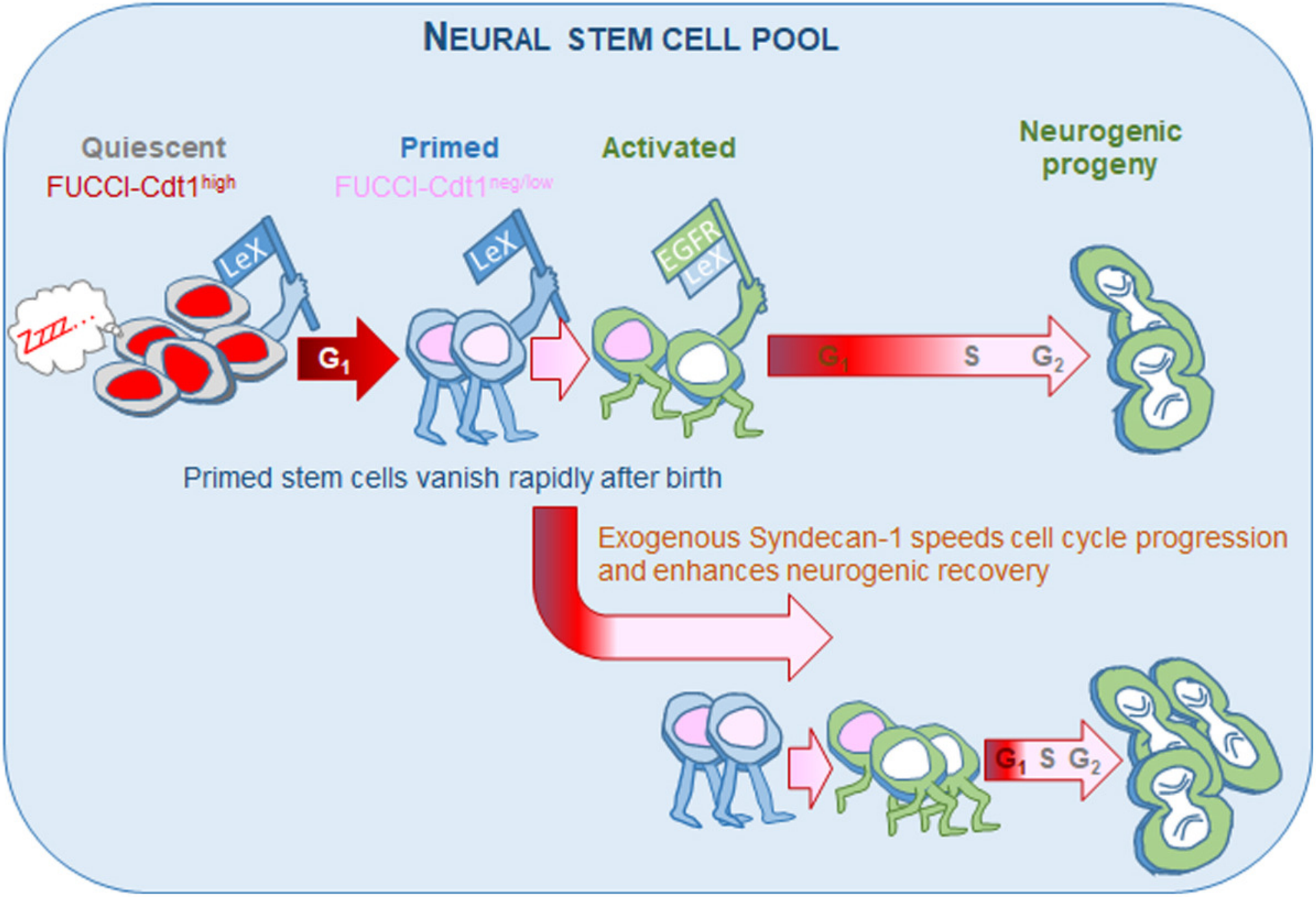
NEURAL STEM CELL POOL
Quiescent
FUCCI-Cdt1high
Primed
FUCCI-Cdt1neg/low
Activated
Neurogenic progeny
LeX
LeX
EGFR
LeX
zzz...
G1
G1
S
G2
Primed stem cells vanish rapidly after birth
Exogenous Syndecan-1 speeds cell cycle progression and enhances neurogenic recovery
G1
S
G2